Asia-Pacific Journal of Science and Technology: Volume: 28. Issue: 06. Article ID.: APST-28-06-20. Research Article

APST

Asia-Pacific Journal of Science and Technology

https://www.tci-thaijo.org/index.php/APST/index

Published by the Research and Graduate Studies,
Khon Kaen University, Thailand

# Thermal and dynamic-mechanical properties of silane functionalized graphene oxide (GO)/Epoxy nanocomposites coatings

Kabiru M. Aujara[1,4,*], Nor A. Ibrahim[1,2,*], Norhazlin Zainuddin[1] , Siti M.M. Nor[1] and Chantara T. Ratnam[3]

[1]Department of Chemistry, Faculty of Science, Universiti Putra Malaysia, Selangor, Malaysia
[2]Materials Processing and Technology Laboratory, Institute of Advanced Technology, Universiti Putra Malaysia, Selangor, Malaysia
[3]Radiation Processing Technology Division, Malaysian Nuclear Agency, Kajang, Malaysia
[4]Department of Science Laboratory Technology, Jigawa State Polytechnic, Dutse, Nigeria
[*]Corresponding author: norazowa@upm.edu.my

Received 23 February 2022
Revised 1 June 2022
Accepted 18 June 2022

**Abstract**

In this study, graphene oxide (GO) and functional-GO (f-GO) were incorporated into epoxy (EP) resins to provide a protective layer for the metal substrate. Functional-GO is synthesized using environmentally friendly gamma irradiation techniques by incorporating methyltriethoxysilane (MTES) to its surface by radiation from gamma-ray. GO, and functionalized-GO are characterized via fourier transform infrared spectroscopy (FTIR), x-ray diffractometer (XRD), and thermogravimetric analysis (TGA). Evidence of silane grafting is indicated by the presence of new peaks in the FTIR spectra of the functionalized GO. The crystal surface changes and surface defects due to modification are determined by XRD. The TGA thermograms showed an increase in weight loss due to the grafting of silane in the 300-650°C associated with the chemically bonded silane degradation on the GO from 0% to 32.17% for GO and TGO-150 respectively. Preparation of the steel substrate protective material begins by ultrasonically dispersing the GO in the solvent before mixing it into an epoxy matrix and adding a hardener. XRD showed the existence of GO morphology and f-GO intercalation and exfoliation throughout the matrix. TGA and dynamic mechanical analysis (DMA) are employed to investigate nanocomposite coatings' thermomechanical properties. The TGA thermogram showed a decrease in percentage weight loss at 350°C ($W_{350°C}$) from 29% for neat epoxy (EP) to 19.8% for ETG-150. Similarly, DMA analysis also showed an increase of Tan δ from 1953.30 MPa to 3414.90 MPa and $T_g$ from 80.18°C to 90.49°C for EP and ETG-150 respectively.

**Keywords:** Epoxy, Graphene oxide, Functionalized-GO, Nanocomposite coatings, Corrosion

## 1. Introduction

Epoxy resins, a thermosetting polymer, fall within the categories of widely used matrices in the composites coatings industries. Features that make epoxy coatings outstanding include good dimensional stability, extreme crosslinking density, high tensile strength, excellent electrical resistance, excellent adhesion to applied substrates, good chemical and thermal stability, excellent intrinsic anti-corrosion (barrier), and reasonable cost [1,3]. However, neat EP used as a barrier in corrosion protection exhibits some disadvantages, such as poor impact resistance, flexibility, poor crack deflection performance, and corrosive agents' permeation due to micro-pore creation during coating fabrication [4]. When these agents such as oxygen, water, and chloride penetrate to substrate/coating interface through these micro-pores, coating properties deteriorate due to adhesion lost [5]. Henceforth, to improve the barrier properties of these coatings, modifications are required. Nanomaterials are favored as a perfect option for improving these barrier properties. Graphene has attracted so much interest due to its exceptional physical and structural properties, such as strength, stiffness, thermal and electrical conductivity [6]. The coatings barrier properties mainly depend on the filler's parameters, such as aspect ratio and dispersion level [7]. Accordingly, graphene oxide (GO) comprises a two-dimensional honeycomb lattice of carbon atoms with functional groups that include hydroxyl and epoxides attached to the basal planes, carbonyl, and carboxyl

groups on the edges [5]. These functional groups assist in the dispersion of GO into the epoxy matrix and provide covalent bonding with the epoxy network [5,8]. Subsequently, the GO's oxygen functional groups make them appropriate grafting sites with organic and inorganic materials [9]. Against this backdrop, GO-based nanofillers have attracted substantial consideration in attaining a higher degree of filler dispersion and deterrence of GO agglomeration due to strong π-π interaction and Van der Waals forces between GO sheets, thereby enhancing effective reinforcement in the polymer matrix, barrier properties against oxygen, water, corrosive ions and superior mechanical strength enhancement [10].

Over the last years, numerous functionalization and surface treatment techniques were employed for enhancing the dispersion and interface of GO and polymer matrix. For instance, various polysiloxane, e.g., organosilane, are commonly used to modify graphene sheets. Through the functionalization process, functional groups such as epoxy, amine, ethylene, thiohydroxy on the silane molecules are attached to the nanofiller's surface. For instance, 3-Aminopropyltriethoxysilane (APTS) was used to functionalize GO by utilizing the amino part and epoxy clusters of GO. Consequently, there is an upsurge in compressive failure strength by ~20% as a result of the addition of 0.1 wt.% APTS-f-G [11]. Similarly, another study shows uniform dispersion and an improvement in yielding strength, Young's modulus, and tensile strength of PE by integration of polyethylene and GO (PE-g-GO) using APTS and maleic anhydride grafted polyethylene at very low loading [12]. APTES functionalized graphene sheet has also shown to improve interfacial interaction and dispersion of graphene sheet in the epoxy matrix with a consequent increase in the tensile property of epoxy composites. It is also found that silane structures grafted on carbon nanotube (CNT) strongly affect CNT/epoxy composite's performance [11]. Li and coworkers functionalized GO via a wash-and-rebuild process with two different silane coupling agents, i.e., 3-Aminopropyltrimethoxysilane (APTMS) and 3-Glycidoxypropyltrimethoxysilane (GPTMS), respectively. The study revealed APTMS-GO and GPTMS-GO have dissimilar reinforcing effects on the composites' mechanical properties; composites containing APTMS-GO exhibit higher Young's modulus and tensile strength while GPTMS-GO filled epoxy composites show a higher increase in ductility [13]. In another study, the effect of pristine GO and silane functionalized-GO (GPTMS-GO) confirms the enhancement of mechanical properties of epoxy composites; the results confirm the improvement is due to covalent bonding between silane-modified GO and epoxy matrix, which enhances interfacial interactions and dispersion in the polymer matrix [14].

Similarly, from a corrosion resistance point of view, APTES functionalized-GO (f-GO) filled in polyvinyl butyral shows improved coating barrier properties [15-16]. In another corrosion study, the effect of GO and APTES-GO on the corrosion resistance of polyurethane coatings are compared; the result shows that GO dispersion in the polymer matrix improves following the modifications, thereby enhancing the anti-corrosion and tribological properties of the polyurethane coatings composites coatings [17].

Herein, the effect of GO and fGO which has excellent properties and are compatible with the epoxy matrix is investigated in the improvement of dynamic-mechanical properties of epoxy resin nanocomposite coatings.

## 2. Materials and methods

### *2.1 Chemicals and reagents*

Graphite powder (<20 μm) supplied by Sigma Aldrich (St. Louis, MO, USA), Hydrogen peroxide ($H_2O_2$, 30%), and sulphuric acid ($H_2SO_4$, 98%) both supplied by Baker Analyzed (Selangor, Malaysia). Hydrochloric acid (HCl, 36%) and potassium permanganate ($KMnO_4$, 99.5%) were acquired from R&M chemicals (Selangor, Malaysia). Methyltriethoxysilane (98%) was obtained from Sigma Aldrich (Selangor, Malaysia), Epoxy resin (diglycidyl ether of bisphenol-A, DGEBA), and polyamide hardener were obtained from Acros Organics reagents (Selangor, Malaysia). Mild steel plates were purchased from Ariff Engineering Works, Selangor, Malaysia. The steel plates were blasted with sandpaper and then washed with deionized water and then finally washed with acetone before coating.

### *2.2 Synthesis of GO and functionalization*

GO is synthesized using graphite powder via the simplified Hummers method. In this method, 3.00 g graphite powder is oxidized by dissolving in 400 mL of concentrated Sulphuric acid ($H_2SO_4$), followed by adding 18.00 g of potassium permanganate ($KMnO_4$). The reaction is allowed to proceed for 72 h under continuous stirring until the graphite is fully oxidized to graphite oxide. The oxidation process was terminated by the addition of a 10% v/v hydrogen peroxide ($H_2O_2$) solution to terminate any excess $KMnO_4$ in the reaction mixture. The resulting GO is washed with aqueous HCl solution (1M) to remove traces of SO42- and then washed with deionized water to removed $Cl^-$ ions. The final product was obtained after freeze-drying.

For the functionalization of GO, a silane solution containing methyltriethoxysilane (MTES) was added to a 50 mL of 2.5 1/gL GO suspension. The mixture is prone sonicated for 1 h. and then stirred for another 30 min before sending for irradiation. Gamma radiation of $^{60}Co$ source with 0.37 MCi activity manufactured by MDS Nordion

Inc, (Ottawa, ON, Canada) with a total dose of 50, 100, and 150 kGy is used for sample irradiation. After irradiation, the mixtures were washed with ethanol and then with water by the centrifugation method for 2 min at 4000 rpm, and the supernatant was then removed. The residue obtained was donated as TGO-150, TGO-100, and TGO-50 were finally washed with a mixture of deionized water and ethanol (60:40 v/v) to remove unreacted silane. The final product was obtained by drying in a freeze dryer.

*2.3 Preparation of nanocomposite coatings*

1wt% of GO and f-GO of the epoxy coating was prepared as follows: First, GO and f-GO were probe sonicated in 50 mL acetone for 1 h; to this suspension, epoxy resin was added and shear mixed with a homogenizer for 30 minutes. The suspension is placed in a vacuum oven at 50-60$^{o}$C for 8 h to remove acetone. Polyamide hardener was mechanically mixed, and the dispersion was coated on a mild steel substrate using a bar coater with a thickness of 150 ± 10 µm. The curing of the coated substrates takes place at room temperature. Nanocomposite coatings prepared for the studies are pure epoxy (EP), GO/Epoxy nanocomposites (EGO), and GO functionalized with APTES at various radiation dosed (50, 100, and 150 kGy) epoxy nanocomposites, i.e., ETG-50, and ETG-100 and ETG-150.

*2.4 Characterizations of GO, f-GO and their nanocomposites*

The fourier transform infrared spectroscopy (FTIR) spectra were recorded using the Perkin Elma spectrum 100 (Waltham, MA, USA). X-ray diffraction was performed by Shimadzu X-ray diffractometer XRD-6000 (Tokyo, Japan) for the GO, f-GO, and nanocomposites at 2Θ = 2° - 50° at the rate of 2°/min. Thermogravimetric analysis was performed with Mettler Toledo 1 HT (Columbus, OH, USA). GO, f-GO and nanocomposites were analyzed from 35°C to 800°C at a heating rate of 10°C/min and nitrogen gas flowing of 20 mL/min. Dynamic mechanical analysis (DMA) is performed by Dynamic Mechanical Analyzer (DMA 3000) Perkin-Elmer. Heating of the samples were carriedout from 30 to 200°C at 2°/min heating rate in single-cantilever mode at a frequency of 1 Hz using oscillation strain of 0.05%. The pencil Hardness test was determined as per ASTM D 3363 to evaluate the film hardness of an organic coating on a substrate.

## 3. Results and discussion

*3.1 Characterization of GO, APTES, and f-GO*

*3.1.1 FTIR and x-ray diffraction (XRD) analysis of GO and f-GO*

The FTIR spectra of GO and f-GO are shown in Figure 1 (A). The GO characteristic peaks are located at 3378,1724, 1634,1359, and 1221 cm$^{-1}$ indicating the presence of hydroxide, epoxide, and carbonyl. Upon functionalization, the characteristics peaks of GO at 1724, 1359, and 1221 cm$^{-1}$ disappear suggesting that the C-O and C-O-C groups of the GO reacted with the silane. Similarly, new peaks in f-GO appear at 2918 and 2865 cm$^{-1}$ corresponding to symmetric and asymmetric vibration of the alkyl groups of the silafune moieties. Also, the presence of peaks at 1123, 1024, and 765 cm$^{-1}$ indicate the formation of Si-O-C, Si-O-Si, and Si-H.

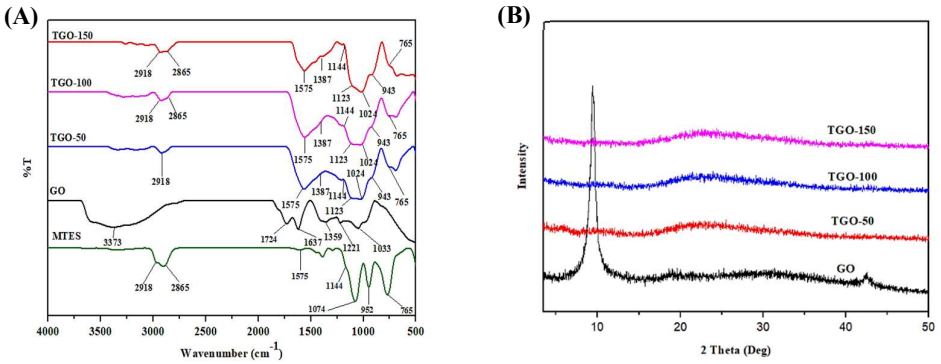


**Figure 1** (A)FTIR (B) XRD spectra of GO, TGO-50, TGO-100 and TGO-150.

XRD pattern of graphite powder exhibits a strong peak at 2Θ=26.5°, a distinctive reflection peak (002) in graphite shows a very high degree of crystallinity with the d-spacing of about 0.34 nm [18]. The intensity of the graphite peak gradually weakens and disappears as the oxidation process proceeds, and this suggests that the

sample becomes amorphous with a less ordered arrangement. Similarly, the diffraction peak at about 2Θ=9.8° appears corresponding to an interlayer spacing increase of graphite from 0.34 nm to 0.90 nm of Graphite Oxide as shown in Figure 1(B). The increase in the graphite oxide interlayer spacing is brought about by the ample covalently bonded oxygen-functional groups between the sheet as a result of the oxidation. The presence of these groups' weakens the forces between the sheets and thus the distance between them increases [19]. The interlayer spacing continues to upsurge upon exposure to the centrifuge process in water; this increase in interlayer depends on the amount of water intercalated within the stacked sheet. Thus, this will further weaken the forces between them and facilitate the formation of individual GO sheets [20]. The centrifuge process also results in the graphitic structure disintegration into fragments [21]. The centrifugation process results in the disappearance of the graphite oxide diffraction peak 2Θ=9.8°, signifying complete graphite oxide exfoliation. The broad peak at the range of 2Θ=20-30° (approx 26°) is attributed to the scattering of water within the aggregate of GO; also, it is interesting to note that the GO aggregate showed a weak diffraction peak at about 2Θ=7-9°, which is lesser than that observed in the diffraction pattern of graphite oxide [21] as shown in Figure 1. GO characteristics XRD peak disappears after functionalization with MTES due to silane moieties intercalations on its surface. These results in the GO's complete exfoliation and its partial reduction, thereby preventing aggregation [22]. Furthermore, a peak appears at around 2Θ = 22.19° with a d-spacing of 0.40 nm, which is significantly lower than that of GO. The decrease in d-spacing results from oxygen-containing groups removal and the overriding effect of silane [22].

*3.1.2 Thermogravimetric (TG) analysis*

The assessment of thermal stability was evaluated based on the decomposition temperature of weight loss from the TG thermogram and to show more evidence of GO functionalization by the silane moieties. Due to its few functional groups, graphite is thermally stable, even at 700°C [14]. Consequent to oxidation, various oxygen functional groups become embedded in the graphene layers and hence decrease the thermal stability of the graphite. GO exhibits the liberation of water as a major decomposition stage of functional groups [23]. Figure 2 depicts the TG and TG derivative (DTG) thermogram of TGO. Typically, GO decomposes in two steps; evaporation of water and decomposition of oxygen functional groups. Considerable loss of water between room temperature and 120°C demonstrates the hydrophilic nature of GO [24] while the second decomposition stage is associated with a major loss within 130-319°C which corresponds to the labile oxygen-containing functionalities decomposition, which indicates GO's low thermal stability. Any weight drop beyond 300°C is associated with more stable functional groups containing oxygen and bulk carbon skeleton pyrolysis [25]. Upon heating GO at a temperature between 30-120°C, GO loses ~19% weight due to the water molecule elimination which is previously adsorbed onto its surface. GO exhibits decomposition behavior (with ~40% weight loss) as the temperature rises from 150-230°C, which is a region attributed to the decomposition of liable oxygen-containing groups. Additional weight loss occurs at a temperature region above 300°C, where 68% weight of GO is lost as a result of pyrolysis of the carbon skeletal [26]. The thermogram shown in Figure 3(A) depicts MTES f-GO thermal behavior (i.e., TGO-150, TGO-100, and TGO-50). It can be seen that all the f-GO exhibits a three-step degradation mechanism within various temperature regions. These regions correspond to where water molecules are lost (0-120°C), a region corresponding to the loss of adsorbed silane on the GO surface and remaining oxygen functional groups are lost (120-300°C), and finally, a region corresponding to thermal decomposition of grafted silane (300-650) [27]. Any further loss of weight above 650°C will be associated with the pyrolysis of the carbon skeletal [23]. With respect to f-GO, the result in Table 1 shows very less weight loss from room temperature up to 148°C, this shows an enhancement in thermal stability and decelerated degradation rate, which is probably due to the grafting of silane on the GO surface. The second degradation temperature which is within 120-300°C is associated with the removal of silane moieties that are physically adsorbed onto the surface of GO while degradation steps within the range of 300-650°C is a region where the actual bond breakage between MTES molecules grafted on the surface of GO. Several studies conducted on graphene and carbon nanotube have pointed out these thermal behaviors [22]. Carbon skeletal pyrolysis described as the end temperature of degradation is shifted significantly to higher temperatures due to silane grafting, which consequently indicates thermal stability [27]. Weight loss (%) of the silanes at various temperature ranges is presented in Table 1.

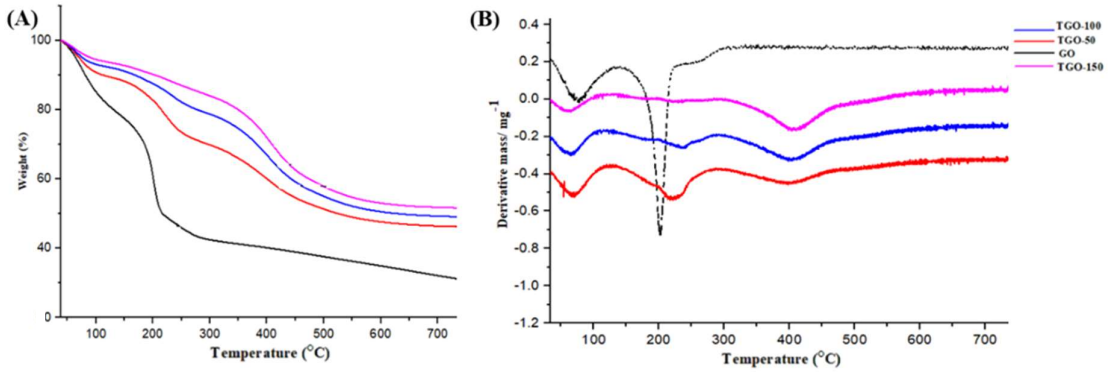


**Figure 2** TG (A) and DTG (B) of GO, TGO-150, TGO-100, and TGO-50.

**Table 1** GO and f-GO percentage weight loss at various temperature regions.

| Samples | Weight loss (%) | | |
|---|---|---|---|
| | 30-120°C | 120-300°C | 300-650°C |
| GO | 18.78 | 39.70 | - |
| TGO-50 | 10.38 | 19.57 | 22.05 |
| TGO-100 | 7.68 | 13.11 | 27.13 |
| TGO-150 | 5.50 | 9.36 | 32.17 |

*3.2 Coatings characterization*

*3.2.1 Scanning electron microscopy (SEM)*

As shown in Figure 3, SEM images of the fracture surface of various EP coatings were employed to show the dispersion and interfacial interaction of GO and f-GO in the EP matrix. Figure 3 (A) below shows the fracture surface of cured neat epoxy resin which exhibits randomly distributed cracks and a smooth surface with river-like patterns (as depicted in the yellow circle) indicating brittle failure [28]. Figure 3 (B) shows EGO (C) ETG-50, (D) ETG-100, and (E) ETG-150 respectively. According to the micrographs, the GO sheet has poor exfoliation in the composites and, therefore, slightly pulled out from the epoxy matrix, indicating a weak interfacial interaction between the GO nanofiller and the epoxy matrix which consequently leads to the agglomeration of the GO layer [29] as seen in the circle in Figure 3 (B). In the case of f-GO filled nanocomposites represented in Figure 3 (C,D, E), the nanocomposites show a homogeneous dispersion.

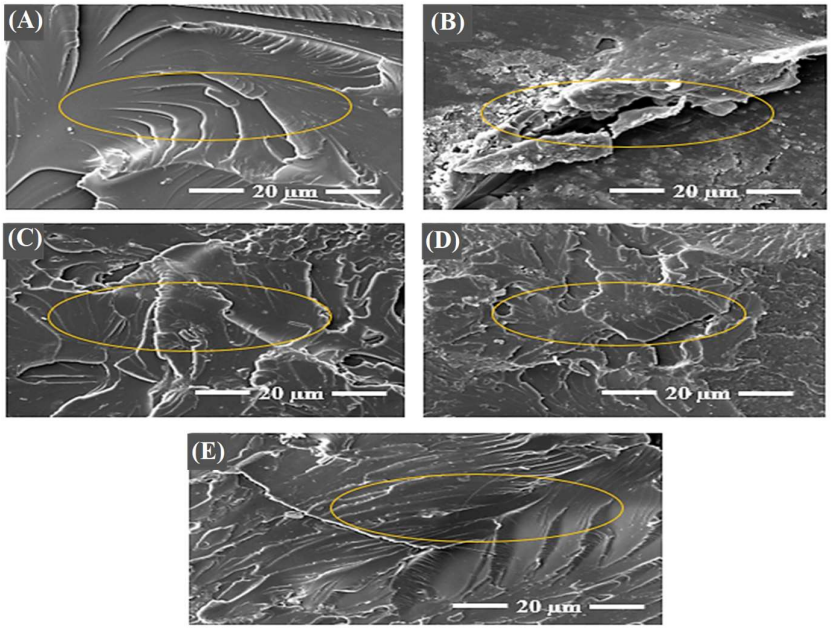


**Figure 3** SEM micrograph of (A) EP, (B) EGO, (C) ETG-50, (D) ETG-100, and (E) ETG-150.

*3.2.2 FTIR*

Epoxy cured by polyamide hardener exhibits characteristic peaks identify as 1511 $cm^{-1}$ (C-C skeletal stretching), 846 $cm^{-1}$ (epoxide ring), and 3380 $cm^{-1}$ (-OH stretching), which confirms the curing of epoxy resin. Inspecting the spectrum of the nanocomposites, i.e., EGO, ETG-50, ETG-100, and ETG-150 in Figure 4, shows that all the functional groups present in the epoxy resin spectrum are present in the nanocomposites, no evidence of the GO band in EGO, ETG-50, ETG-100 and ETG-150 spectrum which is most likely due to the low amount of GO and f-GO and hence, there is no clear dissimilar absorption peak indicating that the interaction is a mere physical than chemical [22].

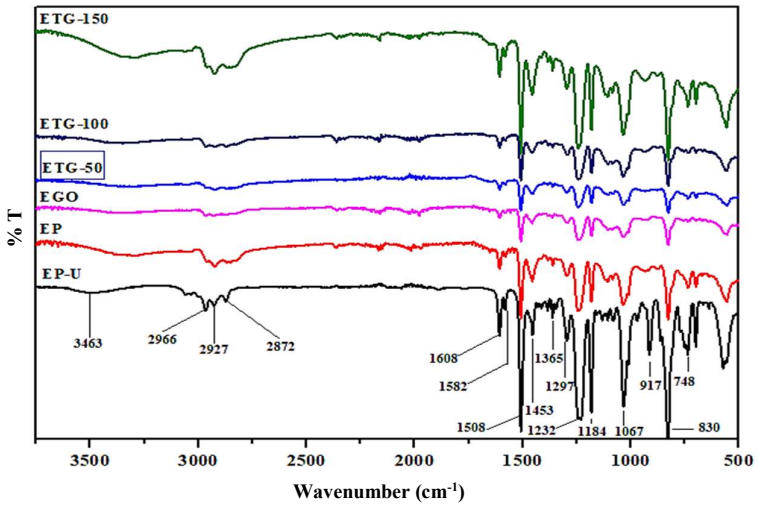


**Figure 4** FTIR of EP, EGO, ETG-50, ETG-100 and ETG-150.

*3.2.3 Hardness properties*

The pencil hardness test is performed because of its ease; it offers a simple scratch output with ease of evaluation at a low cost. Pencil hardness properties are closely related to the scratch resistance [30] while some claim it is related to the tensile strength of the coatings. The hardness of a coating is determined by the pencil grade that does not induce visible damage to the coating. Based on the data compiled in Table 2, it can be seen that the addition of GO and f-GO significantly increases the hardness of the coating. This increase may be attributed to greater compatibility and the high crosslinking density between the GO and f-GO and the polymer matrix [31].

**Table 2** Pencil hardness properties of EP, EGO, ETG-50, ETG-100 abd ETG-150.

| Sampes | Pencil hardness |
|---|---|
| EP | 2H |
| EGO | 3H |
| ETG-50 | 3H |
| ETG-100 | 4H |
| ETG-150 | 4H |

*3.3 Thermal and dynamic-mechanical analysis*

The thermograms for the thermal decomposition of pure epoxy and its nanocomposites are presented in Figure 5. Similarly, numerical data for some specific decomposition temperatures such as onset degradation temperature ($T_{on}$), the temperature at 50% weight loss ($T_{d50\%}$), the temperature of maximum degradation ($T_{dmax}$), mass loss at 350°C ($W_{350°C}$), and residual mass at 500°C ($W_{500°C}$) are presented in Table 3. The samples exhibit a sharp weight-loss stage, which can be associated with the breakdown of the polymer structure [32]. Table 3 shows that the introduction of GO into the epoxy matrix has slightly increased the onset degradation temperature from 328°C for the pure epoxy to 329°C for EGO nanocomposite. Similarly, a decrease in percentage weight loss at 350°C ($W_{350°C}$) from 29% of neat EP to 19.8% for ETG-150 is observed. Moreover, an increase in both temperature of 50% mass loss and temperature of maximum degradation from neat EP to ETG-150 were realized. Again, residual mass at 500°C shows considerable improvement from neat epoxy to MTES f-GO epoxy composites in the order

of ETG-150 >ETG-100 >ETG-50. This shows that the introduction of GO and f-GO nanofiller into the epoxy resin causes a significant increase in the nanocomposites' thermal stability.

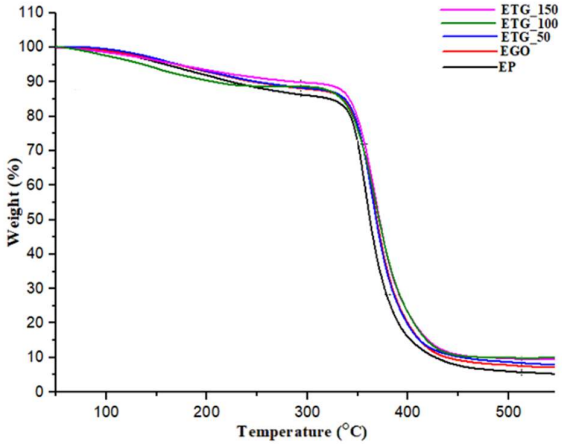


**Figure 5** TG thermograms of EP, EGO, ETG-50, ETG-100 and ETG-150.

The increased decomposition temperature is attributed to the nanofiller's spatial obstruction of the formation of a high crosslinked molecular structure of epoxy. Moreover, graphene is known for its high heat capacity and thermal conductivity [33]. Similarly, the increase in thermal enhancement can be described in terms of GO's dispersion and interfacial interaction with the epoxy matrix [27]. Silane moieties on the surface of GO improve dispersion, thereby restricting the local matrix's mobility within the GO and consequently contributing to an enhanced barrier effect of the f-GO sheets thereby retarding the decomposition of polymer product [26]. Furthermore, an increase in composites' containing silane f-GO residual weight is observed at 500°C. Therefore, the nanocomposites' thermal stability based on MTES f-GO is in the order of ETG-150>ETG-100>ETG-50.

**Table 3** Thermogravimentric parameters of EP, EGO, ETG-50, ETG-100 abd ETG-150.

| Samples | Onset temp of thermal degradation ($T_{on}$) (°C) | Mass loss at 350°C ($W_{350°C}$) (%) | Temerature of 50% mass loss ($T_{50\%}$) (°C) | Temerature of maximum degradation ($T_{max}$) (°C) | Residual mass at 500°C $W_{500°C}$ (%) |
|---|---|---|---|---|---|
| ETG-150 | 338.0 | 19.8 | 373.3 | 435.0 | 13.48 |
| ETG-100 | 333.0 | 20.8 | 369.8 | 427.3 | 9.98 |
| ETG-50 | 331.4 | 21.5 | 369.8 | 420.8 | 8.75 |
| EGO | 329.0 | 21.0 | 368.2 | 417.5 | 6.74 |
| EP | 328.0 | 29.0 | 361.5 | 410.0 | 5.50 |

Dynamic-mechanical analysis techniques illustrate a good indicator of load transfer efficiency in conjunction with chain mobility at the polymer-nanocomposites interface [34,35]. In general, the structure of a material determines its microscopic properties, and therefore its imperative to understand the effect of GO and f-GO on the structure of epoxy coatings. Dynamic Mechanical Analysis (DMA) is used to evaluate the thermochemical behavior of the cured neat epoxy resin and its nanocomposites. Figure 6 (A&B) illustrates the thermomechanical behavior in the form of a DMA plot of storage modulus (E') and damping factor (tan δ) as a function of temperature for neat epoxy (EP), graphene oxide and f-GO nanocomposites and Table 4 summarized the features of storage modulus and tan δ peaks for all the samples in the study. Addition of GO to the neat epoxy results in the increase in the epoxy resin storage modulus. The storage modulus value of the composites containing 1 wt% of GO loading increases from 1953.30 MPa for cured neat epoxy (EP) to 2079.32 MPa for EGO. The highest storage modulus is exhibited by ETG-150 with 3414.90 MPa resulting in an increase of 74% compared to the neat epoxy system. By comparison, a stronger effect is observed by the addition of silane f-GO at various radiation doses to the epoxy matrix. The improvement in the storage modulus can be described by the effect of reinforcement provided by the sheet thereby improving the interfacial interaction due to the introduction of f-GO and restriction in the segmental movement of the epoxy chains [36]. The addition of graphene oxide and f-GO leads to phase formation at the interface between the filler and the matrix, which consequently contributes to energy dissipation from external stress by friction between the filler-filler and filler-polymer at the interface as a result of induced mobility restriction of the local matrix around the sheet [37]. However, as temperature increases,

the storage modulus fall, indicating the dissipation of energy, which took place during the glassy state transition to a rubbery state [23]. For EP, the energy dissipation starts at around 75°C; the same can be said with EGO, which energy of dissipation also begins at around 77°C, this can be attributed to the adsorption of epoxy resin by the oxygen functional groups present on the surface of graphene oxide (GO) or their participation in the curing reaction. This leads to a non-stoicheiometric balance between the epoxy resin and the curing agent [37]. The f-GO nanocomposites' initial transition temperature shift to a higher temperature of about 82-90°C as a result confinement effect, this relaxation occurs at a narrower temperature range, which can be attributed to the enhancement of interfacial interaction between the epoxy matrix and the f-GO as well as lamellar barrier effect of the nano-flakes hindering the segmental motion of the polymer chain in the matrix at a temperature lower than 90°C [32].

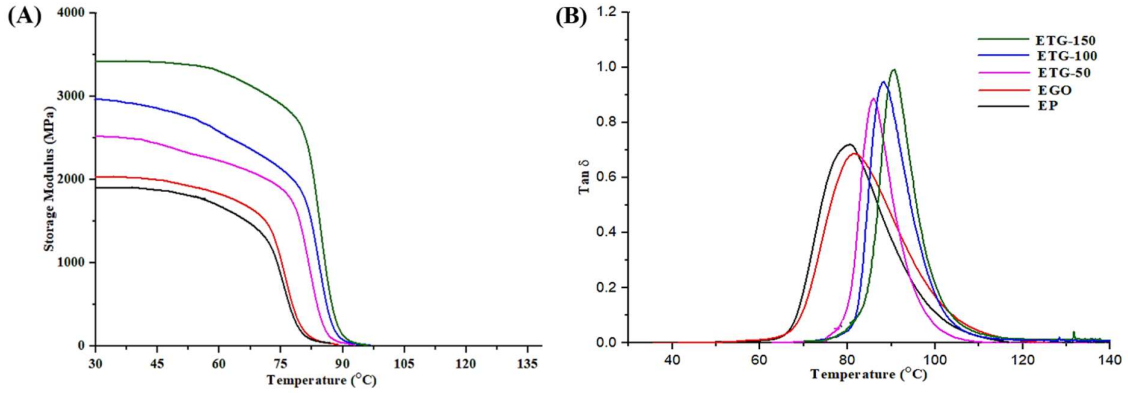


**Figure 6** Storage modulus (E′) and loss factor (tan δ) curves of epoxy and its nanocomposites as a function of temperature for EP, EGO, ETG-50, ETG-100, and ETG-150.

**Table 4** Summary of storage modulus and tan δ.

| Serial No. | Samples | Storage modulus E' (MPa) | $T_{g\ from}$ tan δ (°C) |
|---|---|---|---|
| 1 | EP | 1953.30 | 80.18 |
| 2 | EGO | 2079.32 | 81.24 |
| 3 | ETG-50 | 2530.52 | 85.75 |
| 4 | ETG-100 | 2962.58 | 88.12 |
| 5 | ETG-150 | 3414.90 | 90.49 |

Tan δ is essentially the measure of damping properties of materials and can be obtained by the ratio between the loss modulus and storage modulus [27]. Glass transition temperature ($T_g$) whose value is defined as the peak temperature of the tan δ, is determined from the dumping parameter (tan δ ). Table 3 summarizes the features of tan δ peaks that is the $T_g$. An increase in $T_g$ is observed when graphene oxide (GO) and functionalized graphene oxide (f-GO) are added to epoxy resin, respectively. There is an increase in $T_g$ value of epoxy nanocomposites upon GO and f-GO loading. For instance, there is an increase in $T_g$ from 80.18°C for neat epoxy to 81.24°C when the epoxy resin is filled with 1 wt.% GO indicating significant confinement of the matrix segment [27]. An increase in the glass transition temperature ($T_g$) is more pronounced by the addition of functionalized graphene oxide (f-GO) as depicted in Table 4 . The large surface area of GO sheets and its wrinkled structure may likely results in improved mechanical interlocking with the epoxy matrix, thereby efficiently restricting molecular chain flexibility [37]. Also, the π-π interaction between the aromatic segment of the matrix molecule and that of the GO sheet will lead to the formation of non-covalent bonding in the system [3] and finally, bonding between f-GO and that of the matrix during the curing process may improve the filler-matrix interfacial interaction resulting in conformational alteration of the matrix within the vicinity of the f-GO filler leading to increased thermal resistance [34]. In general, the incorporation of GO and f-GO to the matrix decrease the density of the composites, and since the value of $T_g$ is directly related to the crosslinking density in this type of network structure, it is expected that segmental mobility will be inhibited, which leads to increase of free volume and consequently increase in $T_g$ and storage modulus (E') [3].

## 4. Conclusion

MTES was grafted onto the surface of GO, and the resultant f-GO was dispersed into epoxy resin to obtain f-GO/epoxy nanocomposites coatings via sonification and shear mixing. The disappearance of GO's hydroxyl, carboxyl, and epoxied groups with the sudden appearance of Si-O-C, Si-O-Si, Si-H, and Si-O-C in the FTIR spectra provide evidence of GO functionalization. Similarly, other characterization techniques such as FTIR and XRD further verified the success of the functionalization of GO. Furthermore, the morphology of the prepared nanocomposites coatings was investigated by XRD and SEM, which proved the successful deployment of f-GO into the epoxy matrix. The functionalization of GO significantly influences the dispersion of graphene layers in the epoxy resin matrix as depicted in the XRD diffractogram. All the prepared nanocomposite coatings show significant improvement in the thermal properties compared to neat epoxy owing to a good dispersion state of f-GO (i.e., ETG-150, ETG-100, and ETG-50) with ETG-150 exhibiting more efficient improvement. Moreover, the filled polymer interfacial interaction of the nanocomposites was studied by DMA. The results also indicate an increased storage modulus, and glass transition temperature ($T_g$) for the nanocomposites compares to the neat epoxy.

## 5. Acknowledgments

The authors will like to thank the Fundamental Research Grant Scheme, Ministry of Education Malaysia, grant number 5524950 for funding this research.

## 6. References

[1] Ramezanzadeh M, Ramezanzadeh B, Gahlakeh G, Tati A, Mahdavian M. Development of an active/barrier bi-functional anti-corrosion system based on the epoxy nanocomposite loaded with highly-coordinated functionalized zirconium-based nanoporous metal-organic framework (Zr-MOF). Chem Eng J. 2021;408:127361.

[2] Muralishwara K, Kini UA, Sharma S. Epoxy-clay nanocomposite coatings: a review on synthesis and characterization. Mater Res Express. 2019;6(8):1-8.

[3] Haeri M, Ramezanzadeh M, Ramezanzadeh B. Ce-TA MOF assembled GO nanosheets reinforced epoxy composite for superior thermo-mechanical properties. J Taiwan Inst Chem Eng. 2021;126:313-323.

[4] Ramezanzadeh M, Tati A, Bahlakeh G, Ramezanzadeh B. Construction of an epoxy composite coating with exceptional thermo-mechanical properties using Zr-based $NH_2$-UiO-66 metal-organic framework (MOF): experimental and DFT-D theoretical explorations. Chem Eng J. 2021;408:127366.

[5] Zheng H, Shao Y, Wang Y, Meng G, Liu B. Reinforcing the corrosion protection property of epoxy coating by using graphene oxide-poly(urea-formaldehyde) composites. Corros Sci. 2017;123:267-277.

[6] Rajitha K, Mohana KNS, Mohanan A, Madhusudhana AM. Evaluation of anti-corrosion performance of modified gelatin-graphene oxide nanocomposite dispersed in epoxy coating on mild steel in saline media. Colloids Surfaces A: Physicochem Eng Asp. 2020;587:124341.

[7] Pourhashem S, Vaezi MR, Rashidi A, Bagherzadeh MR. Distinctive roles of silane coupling agents on the corrosion inhibition performance of graphene oxide in epoxy coatings. Prog Org Coatings. 2017;111:47-56.

[8] Ramezanzadeh M, Ramezanzadeh B, Mahdavian M, Bahlakeh G. Development of metal-organic framework (MOF) decorated graphene oxide nanoplatforms for anti-corrosion epoxy coatings .Carbon. 2020;161:231-251.

[9] Cui G, Bi Z, Zhang R, Liu J, Yu Xin, Li Z. A comprehensive review on graphene-based anti-corrosive coatings. Chem Eng J. 2019;373:104-121.

[10] Bhardiya SR, Asati A, Sheshma H, Rai A, Rai VK, Singh M. A novel bioconjugated reduced graphene oxide-based nanocomposite for sensitive electrochemical detection of cadmium in water. Sens Actuators B Chem. 2021;328:129019.

[11] Özmen EN, Kartal E, Turan MB, Yazıcıoğlu A, Niazi JH, Qureshi A. Graphene and carbon nanotubes interfaced electrochemical nanobiosensors for the detection of SARS-CoV-2 (COVID-19) and other respiratory viral infections: a review. Mater Sci Eng C. 2021;129:112356.

[12] Tian J, Xu T, Tan Y, Zhang Z, Tang B, Sun S. Effects of non-covalent functionalized graphene oxide with hyperbranched polyesters on mechanical. Materials. 2019;12(19): 3103.

[13] Shivakumar H, Renukappa NM, Shivakumar KN, Suresha B. The reinforcing effect of graphene on the mechanical properties of carbon-epoxy composites. Open J Compos Mater. 2020;10(2):27-44.

[14] Altin Y, Yilmaz H, Unsal OF, Bedeloglu AC. Graphene oxide modi fied carbon fiber reinforced epoxy composites. 2020;40(5):415-420.

[15] Kausar A. Corrosion prevention prospects of polymeric nanocomposites: a review. J Plast Film Sheeting. 2019;35(2):181-202.
[16] Aujara KM, Chieng BW, Ibrahim NA, Zainuddin N, Ratnam CT. Gamma-irradiation induced functionalization of graphene oxide with organosilanes. Int J Mol Sci. 2019;20(8):1910.
[17] Deyab MA. Anticorrosion properties of nanocomposites coatings: a critical review. J Mol Liq. 2020;313:113533.
[18] Hu H, Zhao S, Sun G, Zhong Y, Bo Y. Evaluation of scratch resistance of functionalized graphene oxide/polysiloxane nanocomposite coatings. Prog Org Coatings. 2017;117:118-129.
[19] Gao W. Synthesis, structure, and characterizations. In Gao W, editor. Graphene oxide reduction recipes, spectroscopy and applications. 1st ed. New York: Springer Publishing; 2015.
[20] Dimiev AM, Shukhina K, Khannanov A. Mechanism of the graphene oxide formation: the role of water, 'reversibility' of the oxidation, and mobility of the C-O bonds. Carbon. 2020;166:1-14.
[21] Zhang W, Wei L, Ma J, Bai SL. Exfoliation and defect control of graphene oxide for waterborne electromagnetic interference shielding coatings. Compos Part A Appl Sci Manuf. 2020;132:105838.
[22] Chen C, He Y, Xiao G, Zhong F, Xia Y, Wu Y. Graphic C3N4-assisted dispersion of graphene to improve the corrosion resistance of waterborne epoxy coating. Prog Org Coat. 2019;139:105448.
[23] Wu W, Xu Y, Wu H, Chen J, Li M, Chen T, et al. Synthesis of modi fi ed graphene oxide and its improvement on fl ame retardancy of epoxy resin. J Appl Polym Sci. 2019;137(1)1-11.
[24] Ma WS, Li J, Deng BJ, Zhao XS. Preparation and characterization of long-chain alkyl silane-functionalized graphene film. J Mater Sci. 2013;48(1):156-161.
[25] Zhu Y, Murali S, Cai W, Li X, Suk W, Potts JR, et al. Graphene and graphene oxide: synthesis, properties, and applications. Adv Mater. 2010;22(135):3906-3924.
[26] Liu H, Pang X, Ding W, Guo S, Ding Z. Preparation of nano-$SiO_2$ modified graphene oxide and its application in polyacrylate emulsion. Mater Today Commun. 2021;27:102245.
[27] Khan NI, Halder S, Talukdar N, Das S. Surface oxidized/silanized graphite nanoplatelets for reinforcing an epoxy matrix. Mater Chem Phys. 2021;258:123851.
[28] Qu L, Sui Y, Zhang C, Li P, Dai X, Xu B, et al. POSS-functionalized graphene oxide hybrids with improved dispersive and smoke-suppressive properties for epoxy flame-retardant application. Eur Polym J. 2020;122:109383.
[29] Bouibed A, Doufnoune R. Synthesis and characterization of hybrid materials based on graphene oxide and silica nanoparticles and their effect on the corrosion protection properties of epoxy resin coatings. J Adhes Sci Technol. 2019;33(8):834-860.
[30] Da Y, Liu J, Gao Z, Xue X. Studying the influence of mica particle size on the properties of epoxy acrylate /mica composite coatings through reducing mica particle size by the ball-milled method. 2022;12(1):1-15.
[31] Relosi N, Neuwald OA, Zattera AJ, Piazza D, Kunst SR, Birriel EJ. Effect of addition of clay minerals on the properties of epoxy/polyester powder coatings. Polimeros. 2018;28(4):355-367.
[32] Khezri T, Sharif M, Pourabas B. Polythiophene-graphene oxide doped epoxy resin nanocomposites with enhanced electrical, mechanical and thermal properties. RSC Adv. 2016;6(96):93680-93693.
[33] Rehim MA, Turky G. Silane-functionalized graphene oxide/epoxy resin nanocomposites: Dielectric and thermal studies. J Appl Polym Sci. 2019;136(47):1-11.
[34] Ramezanzadeh M, Bahlakeh G, Ramezanzadeh B. Construction of an epoxy composite with excellent thermal/mechanical properties using graphene oxide nanosheets reduced/functionalized by *Tamarindus indiaca* extract/zinc ions; detailed experimental and DFT-D computer modeling explorations. Results Phys. 2020;19:103400.
[35] Ferreira FV, Brito FS, Franceschi W, Simonetti EAN, Cividanes LS, Chipara M, et al. Functionalized graphene oxide as reinforcement in epoxy based nanocomposites. Surf Interfaces. 2018;10:100-109.
[36] Ramezanzadeh M, Bahlakeh G, Ramezanzadeh B. Green synthesis of reduced graphene oxide nanosheets decorated with zinc-centered metal-organic film for epoxy-ester composite coating reinforcement: DFT-D modeling and experimental explorations. J Taiwan Inst Chem Eng. 2020;114:311-330.
[37] Sharma H, Kumar A, Rana S, Guadagno L. An overview on carbon fiber-reinforced epoxy composites : effect of graphene oxide incorporation on composites performance. 2022;14(8):1-21.